Habitat International 158 (2025) 103350

Contents lists available at ScienceDirect

Habitat International

journal homepage: www.elsevier.com/locate/habitatint

Inferring ghost cities on the globe in newly developed urban areas based on urban vitality with multi-source data

Yecheng Zhang, Tangqi Tu, Ying Long *

School of Architecture, Tsinghua University; Hang Lung Center for Real Estate, Tsinghua University; Key Laboratory of Ecological Planning & Green Building, Ministry of Education, Tsinghua University, Beijing, 100084, China

ARTICLE INFO

Keywords:
Ghost cities
Urban vitality
Sustainable urbanization
Multi-source data

ABSTRACT

Due to rapid urbanization over the past 20 years, many newly developed areas have lagged in socio-economic maturity, creating an imbalance with older cities and leading to the rise of "ghost cities". However, the complexity of socio-economic factors has hindered global studies from measuring this phenomenon. To address this gap, a unified framework based on urban vitality theory and multi-source data is proposed to measure the Ghost City Index (GCI), which has been validated using various data sources. The study encompasses 8841 natural cities worldwide with areas exceeding 5 km^2, categorizing each into new urban areas (developed after 2005) and old urban areas (developed before 2005). Urban vitality was gauged using the density of road networks, points of interests (POIs), and population density with 1 km resolution across morphological, functional, and social dimensions. By comparing urban vitality in new and old urban areas, we quantify the GCI globally using the theory of urban vitality for the first time. The results reveal that the vitality of new urban areas is 7.69% that of old ones. The top 5% (442) of cities were designated as ghost cities, a finding mirrored by news media and other research. This study sheds light on strategies for sustainable global urbanization, crucial for the United Nations' Sustainable Development Goals.

1. Introduction

1.1. Research background

Due to urbanization in many countries, rapid urban land expansion has become a global phenomenon (Li et al., 2020a; Liu et al., 2020; Wang et al., 2022). Especially in emerging economies and developing countries, numerous new urban areas have been built up. Yet, it is crucial to emphasize that the rate of urban socioeconomic progress has not paralleled this land expansion. Many new urban areas are thus inadequately developed at a low socioeconomic level, resulting in abundant vacancies in these new urban areas described as so-called "ghost cities" (Jin et al., 2017). 'Ghost cities' traditionally describe urban areas abandoned due to factors like resource depletion or market shifts (Constant, A. F. & Zimmermann, K. F., 2013; Roger S. A., 2011). However, recent studies, especially by Xu (2022), highlight a shift in understanding, emphasizing newly built but uninhabited areas, especially in developing regions. The United Nations' Sustainable Development Goal 11 (SDG11) is to make cities inclusive, safe, resilient, and sustainable (United Nations, 2015), and ghost cities are always generally considered to have negative impacts on developing sustainable cities (Batty, 2016). To cope with ghost cities and achieve SDG11, it is essential to explore the existence of ghost cities and identify their characteristics on a global scale.

Understanding the definition of ghost cities is foundational to their identification. Some scholars have defined this term from various perspectives. The concept of "ghost cities" or "ghost estates" was originally proposed to describe vacant housing in Ireland (O'Callaghan et al., 2014), which means the original ghost cities were once inhabited but became empty after the people left. However, with the rapid growth of cities globally in recent times, the term "ghost city" has been redefined from a new perspective, beginning to refer to the phenomenon of high vacancy rates, shrinking commercial activities, and sparse population in newly built urban areas due to over-development and improper planning (Williams et al., 2019). Shepard (2015) describes a "ghost city" as "a new development that is running at significantly under capacity, a place with drastically fewer people and businesses than there is an available space for". Moreover, he elaborates on some phenomena that have appeared in Chinese cities as a typical warning of today's ghost cities. With the continuous development of data and technology, ghost

* Corresponding author.
E-mail addresses: zhangyec23@mails.tsinghua.edu.cn (Y. Zhang), tutangqi@mail.tsinghua.edu.cn (T. Tu), ylong@tsinghua.edu.cn (Y. Long).

https://doi.org/10.1016/j.habitatint.2025.103350
Received 8 August 2024; Received in revised form 10 February 2025; Accepted 19 February 2025

cities in new urban areas have evolved in their definitions. These "ghost cities" in new urban areas generated from urban expansion have drawn concerns widely from scholars, social media, and governments (Batty, 2016; Jiang et al., 2015; Zheng et al., 2017). Therefore, this study primarily focuses on ghost cities from the perspective of the inadequate operating level of newly built-up urban land.

1.2. Literature review

Strictly identifying a city as a 'ghost city' is complex, especially on a global scale. Some researchers explored identifying and evaluating ghost cities on a local scale. In these studies, ghost cities are mainly identified and evaluated based on population (Leichtle et al., 2019; Zhang et al., 2022a), firms (Dong et al., 2021), nighttime satellite image data (Shi et al., 2020; Zheng et al., 2017, 2019), and amenities (Williams et al., 2019). On the one hand, these local scale analyses based on population or built environment indicators identified ghost cities defined by thresholds chosen without considering the consistency across geographical regions. That's to say such a threshold is usually suitable for a local homogeneous geographical scale, and there are huge differences in urban construction between different geographical regions in the world. On the other hand, previous studies have revealed that ghost cities have been existing in the new urban areas of some specific cities or some major countries like the United States and China. Nevertheless, whether ghost cities exist widely in the world and how to identify them at the global scale remain in question, which is important for global sustainable urbanization, especially in many developing countries experiencing rapid urbanization. It is thus necessary to establish an effective framework to identify global ghost cities based on related theories at a more sophisticated level with multi-source data.

Furthermore, while a unified standard for defining ghost cities remains elusive (Jin et al., 2017; Shi et al., 2020), their hallmark of low spatial vitality in new urban regions is evident (Ge et al., 2018). This study leverages urban vitality theory to identify global ghost cities by comparing the vitality of newer urban areas with that of older ones. Lynch posits urban vitality as a metric of urban space quality, crucial for settlements that cater to human needs and ensure species survival (Lynch, 1984). When assessing this vitality, numerous researchers utilize indicators related to 'urban form', 'life place', and 'human activity', concepts introduced by both Jacobs (1961) and Lynch (1984). These indicators capture critical urban design elements (Long & Huang, 2019). Urban vitality often parallels a high 'quality of life'. Jacobs underscores the interplay between human activity and life space, suggesting that a city's vitality reflects its diverse life. Building on these theories, this study decomposes urban vitality into three key elements for calculation using accessible data: the morphological, functional, and social dimensions of urban vitality. As highlighted by Jin et al. (2017), urban vitality forms the foundation for a quality urban life, derived from good urban form, developed urban functions, and sufficient urban activities. In this way, the relative vitality inadequacy of new urban areas can be presented when compared with corresponding old urban areas, characterized by limited secondary functions, fewer small blocks and corners, a lack of mixed-age buildings, and lower population density, thereby providing the quantitative foundation for identifying ghost cities. Moreover, beyond the urban vitality theory, there exist other indicators with globally comparable datasets, and this study has conducted comparative analyses using these indicators, as detailed in the section Calculation of GCI and Supplementary Information.

Building upon the theoretical framework, this study delves into the specific dimensions of urban vitality through an extensive literature review. The morphological dimension, represented by "urban form", is influenced by factors such as development density, providing the physical environment for urban vitality (Kropf, 2017; Akinci et al., 2022; Chen, Dong, et al., 2022; Gu et al., 2023; Li et al., 2023; Wang et al., 2024; Wu et al., 2018; Ye et al., 2018; Zhang et al., 2022b, 2022c). Aligned with Jacobs's (1961) assertion, road density and the presence of small blocks with frequent corners enhance accessibility and promote social interactions, thereby increasing morphological vitality. The functional dimension, or "life place", is driven by economic development, where higher levels of economic activity lead to diverse urban functions that enhance urban utilization (Chen et al., 2022; Huang et al., 2020; Yue et al., 2021). Incorporating Jacobs's (1961) concept of secondary functions, functional vitality is measured by the diversity of land uses that ensure continuous activity and economic viability throughout different times of the day. The social dimension, or "human activity", is reflected in the spatial concentration of populations, with increased social interactions fostering greater urban vitality (Guo et al., 2022; Sung et al., 2013; Zhou, 2012). Consistent with Jacobs's (1961) emphasis on concentration, social vitality is quantified using population density data, which indicates the potential for rich social interactions and economic activities within urban spaces. These dimensions are operationalized through specific indicators: road density measures morphological vitality by increasing accessibility and potential for urban activities (Paköz et al., 2022; Yue et al., 2021); POIs density captures functional vitality by detailing the types and locations of urban functions (Delclòs-Alió & Miralles-Guasch, 2018; Dong et al., 2021; Gómez-Varo et al., 2022; Jiang et al., 2015; Williams et al., 2019; Yue et al., 2021); and population density represents social vitality by indicating the concentration of human interactions within urban spaces (Dong et al., 2021; Gowharji, 2016; Jin et al., 2017; Leichtle et al., 2019; Shi et al., 2020; Zhang et al., 2022a; Zheng et al., 2017, 2019). By integrating Jacobs's (1961) conditions for diversity and concentration into these indicators, and considering the limitations in obtaining comprehensive data that fully aligns with Lynch's detailed urban vitality indicators, the study quantitatively assesses the urban vitality of new versus old urban areas, thereby providing a robust framework for the identification of ghost cities based on relative vitality inadequacies.

1.3. Problem statement and objectives

Given the paramount importance of identifying global ghost cities for policy formulation, urban planning, and sustainable urbanization, there's an urgent need to establish a quantifiable and universally comparable framework. Although many studies have been done to predict ghost cities in a local area through indicators such as population distribution and built environment, these methods are not extensible on a global scale. Therefore, the main innovation of this study is constructing an effective framework to identify global ghost cities based on urban vitality differences with more sophisticated methods and more accessible data. In this article, we derive 8841 natural cities through the data of urban boundaries in 2005 and 2018 (Li et al., 2020a; Xu et al., 2021) at first, which we refer to as "natural cities" throughout this article. By dividing natural cities into new urban areas (developed after 2005) and old urban areas (developed before 2005), we borrow the urban vitality theory to measure the vitality gap between the new and old urban areas in the natural cities with 1 km resolution, calculating the GCI and infer the distribution of ghost cities in newly developed urban areas. Referring to this, we also analyzed the characteristics of global ghost cities in various countries and regions. Subsequently, we verified our identified results in different scales using Google search engines and related research, which showed consistent results. At the same time, in order to understand the spatial distribution pattern of the GCI in this paper, the demographic factors have been considered in the research, and verified our results through the actual population growth of natural cities. The ghost city index we gave illustrated a strong potential to overcome the difference in urban scales across cities on the globe. Using this unified framework, we can discuss the possibility of the widespread distribution of new urban areas in the natural cities on the globe and observe differences in scale at the intercontinental, national, and urban levels in a quantitative manner. Our result can provide a scientific reference for global urban planning to achieve sustainable urbanization.

2. Methodology

2.1. Methodology framework

We used a unified spatial analysis unit to aggregate data from different dimensions to calculate the vitality index of new and old urban areas for each natural city and obtained the GCI for each natural city using the corresponding formula. The three dimensions of measuring urban vitality include morphological, functional, and social dimensions. Based on the literature review mentioned above, we selected road network density, POIs density, and population density to represent the three dimensions, respectively. These indicators can be further supported by more accurate and open data in the future to analyze more detailed scale. Our method includes three steps: (1) Data preprocessing: Based on interpreted remote sensing products (Li et al., 2020a; Xu et al., 2021) GHUB and GUB data, globally comparable natural city expansion data were obtained through geospatial matching (see section 2.3 Data acquisition and 2.4 Global urban areas). At the same time, the global population, POIs and road network data are collected and unified to the 1-km grid. With further unification of urban definitions by the United Nations, urban boundary data will become more available (Li, Zhang, Li, & Long, 2024). (2) Calculation of the ghost city index: Indicators for the three dimensions and urban vitality of new and old urban areas were calculated, and then the ghost city index for each natural city was derived and analyzed at global, intercontinental, national, and urban scales (see section 2.2 Calculation of GCI). (3) Validation of calculation results: Validation was conducted at two levels. First, by scraping Google keyword searches, we obtained the popularity rankings of ghost city search terms for countries and regions globally and compared them with our results. Second, we calculated population and land expansion for all natural cities across different years to verify whether the inference of ghost cities based on the demographic factor from new and old urban areas is reasonable (see section 3.5 Benchmarking our results from news media and related research and 3.6 Understanding the distribution of GCI from different perspective) (see Fig. 1).

2.2. Calculation of GCI

In terms of measuring the vitality of urban areas, a straightforward quantitative method is employed to measure the vitality of all the urban areas on the globe (Jin et al., 2017). First, the density distribution layers of road junctions, POIs and population are calculated and generated by the software ArcGIS. Each output raster is set with a cell size of 1 km to maintain the consistence of these three layers covering the entire world. The second step is to measure the average value of each layer within each urban area. Finally, the vitality of each urban area is measured by the equation below:

$$V = M^{*}F^{*}S \quad (1)$$

where V is the vitality; M is the density of road network as the indicator from the morphological dimension; F is the density of POIs as the indicator from the functional dimension; S is the population density as the indicator from the social dimension. This equation indicates that an urban area with denser roads, more urban functions and more human activities tends to have a higher vitality level.

Based on the results of measuring the vitality of global urban areas, the ghost city index of new urban areas can be calculated for all the cities on the globe by combining the vitality values of the new and old urban areas in each city. The equation that can be used is (Jin et al., 2017):

$$GCI = 1 \ / \ (V_{new} \ / \ V_{old} * V_{new}) \quad (2)$$

where GCI is the ghost city index of the new urban area in a city; V_{old} is the average vitality of all the grids in the old urban area in a city; V_{new} is the average vitality of all the grids in the new urban area in a city. According to this equation, the ghost city level of the new urban area that a city belongs to is associated with the vitality of the new urban area and the vitality difference between new and old urban areas in the city. If the vitality of the new urban area is lower or the vitality difference between new and old urban areas is larger, this index will be higher and the new urban area of the city is more likely to be a so-called “ghost city” (Jin et al., 2017). All the cities can be then ranked based on this index to identify ghost cities by higher index values.

Additionally, the sufficiency and necessity of the selected indicators

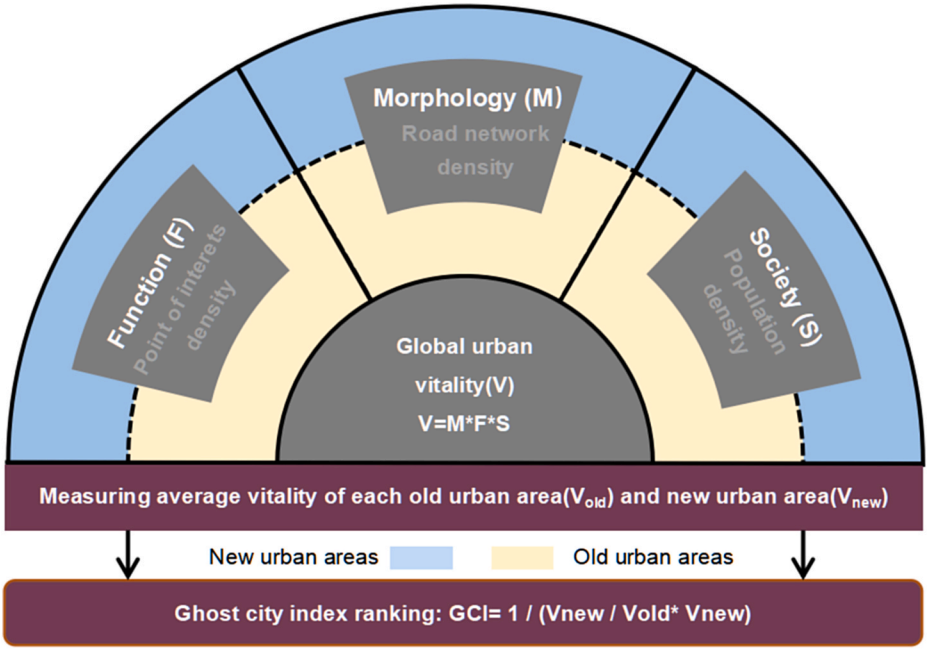

Fig. 1. Methodological framework of this study. The degree to which a city belongs to a ghost city is related to vitality in new urban areas and the difference in vitality between old and new urban areas. The larger the difference and the lower the vitality in the new residential projects, the more likely the city to be a ghost city.

representing the vitality theory need to be further elucidated, particularly considering the differences in data quality across regions within global datasets (Huang et al., 2023). By analyzing the correlation between population density, road density and POIs density and night lighting data, this study verifies the sufficiency and necessity of these three indicators in measuring urban vitality (Aubrecht et al., 2016; Elvidge et al., 2021; Store, 2019; Xia et al., 2022) (see Supplementary Note2). Although morphological and ecological characteristics are often considered in urban analysis, it is found that these variables have limited improvement on the model, but increase the complexity. In addition, by introducing ecological factors such as cultivated land, forest and grassland, it is found that there is a contradiction between the inverse vitality index and the traditional GCI, indicating that the inverse identification method may not be suitable for accurately evaluating the ghost city phenomenon.

2.3. Data acquisition

Multi-source data were acquired to support this study. The data used for the analysis include global urban boundaries, density of road network, density of points of interest (POIs) and population density. The basic information about the resolution, temporal domain, type and source of the data is shown in Table 1. The detailed description of the data is as follows. The road data and POIs data used in this paper are all from OpenStreetMap(OSM). As an open-source geographic database that is considered as the infrastructure network is nearing completion, OSM provides the only publicly licensed data sources such as geospatial roads, POIs and building footprints at the global level. Many studies have tried to evaluate the data integrity and usability of OSM, Including different scales such as cities, regions and the world, proves the availability of road data and POIs data, especially now (Klinkhardt et al., 2023; Pinho et al., 2023; Oostwegel et al., 2023; Barrington-Leigh & Millard-Ball, 2017; Biljecki et al., 2023; Herfort et al., 2023; Ding et al., 2025).

2.4. Global urban areas

The spatial distribution of global urban areas was determined based on data from two related studies (Li et al., 2020a; Xu et al., 2021) which used global hierarchical urban boundaries (GHUB) and global urban boundaries (GUB) from 2018 to 2005, respectively. Both datasets employed the widely used definition of urban boundary, which was identified using the same 30m global artificial impervious area (GAIA) data with a mean overall accuracy higher than 90% (Gong et al., 2020). New urban areas in this study refer to those developed between 2005 and 2018, while old urban areas refer to those developed before or in 2005. Due to the complexity of urban land changes over time, we adopted a "converting time to space" approach to compare urban areas built in different years within the same city (Fig. 2). We used the urban boundaries in 2018 as the benchmark spatial analysis units, allowing for the division of global new urban areas (GNUA) and global old urban areas (GOUA) within a city for year-to-year comparisons based on observed built-up years.

We chose GHUB instead of GUB in 2018 for two primary reasons. Firstly, GHUB data displays better consistency in urban boundary levels with lower fragmentation characteristics, negating the need to screen for natural city thresholds again. Additionally, GHUB data offers smoother, continuous boundary contours and a more comprehensive analysis of urban components compared to GUB. Our research solely evaluates urban land expansion, eliminating data on the physical shrinkage of urban land. As per this principle, we utilized ArcGIS software to connect, fuse, and remove new city data from 2005 without the old city based on the 2018 city boundary data. Fig. 8 represents only typical expansion situations of urban land, excluding shrinkage circumstances.

Our analysis considered global urban boundary delineations for 2005 and 2018, with 9862 cities initially designated. After data cleaning (appendix), 8841 natural cities were retained as benchmarks, totaling 750,800 square kilometers of area in 2018. Compared to other datasets, our dataset is more accurate and efficient in representing global urban boundaries' spatial details. For example, our dataset highlights more urban fringe areas detail than night-time light-derived data, while maintaining similar urban dynamic consistency (Zhou et al., 2018). The dataset aligns well with human-interpreted data in terms of overall spatial distribution and spatial details around urban fringe areas, reducing intensive human labor (Wang et al., 2012). Our dataset reflects the actual spatial extent and urban dynamics for large and small cities globally, making it internationally comparable (Xu et al., 2021).

Table 1
Basic information of the data used in this study.

Name	Temporal domain	Type	Source
Global urban boundaries	2018, 2005	Polygon	Li et al., 2020a; Xu et al., 2020; (http://data.ess.tsinghua.edu.cn/; https://doi.org/10.5281/zenodo.5168383)
Density of road network	2022	Polyline	OpenStreetMap (http://download.geofabrik.de/)
Density of points of interest (POIs)	2022	Point	OpenStreetMap (http://download.geofabrik.de/)
Population density	2020/2005	Raster/1 km resolution	WorldPop unconstrained global population grids (https://www.worldpop.com/)
National boundaries	2022	Polygon	OpenStreetMap (http://download.geofabrik.de/)
Multilevel administrative boundaries	2022	Polygon	Database of Global Administrative Areas (GADM, https://gadm.org/)

2.5. Density of road network

In this study, we harnessed global road network data from OpenStreetMap to assess morphological urban vitality globally using road network density as a metric. According to the visual interpretation and evaluation of satellite images, some researchers have proved that 83% of the global road data of OSM in 2017 has been completed, and more than 40% of countries have complete road networks (Barrington-Leigh & Millard-Ball, 2017). The road network data, collected on February 1st, 2022, demonstrates consistent comparability across cities spanning various countries and regions. Using spatial analysis tools within the ArcGIS software, we processed this data to visualize the global distribution of road network density. Integrating it with global urban area data, we derived road network density figures for both old and new urban areas on a global scale.

2.6. Density of POIs

To measure global functional urban vitality based on the density of POIs, we collected global POIs data from OpenStreetMap, similar to the data source for road network density. The data collection date was February 1st, 2022. Researchers have proved that POIs data in osm after 2020 is more comprehensive, and there is a high correlation between the counting POIs mode and the statistics of Google Street View in several European cities (Pinho et al., 2023). Considering OSM provides the only publicly licensed data sources, the POIs data used in this paper comes from the OSM in 2022. Using this data and global urban area data, we calculated the density of POIs for old and new urban areas at a global scale.

2.7. Population density

Population density refers to the number of people per unit area. To

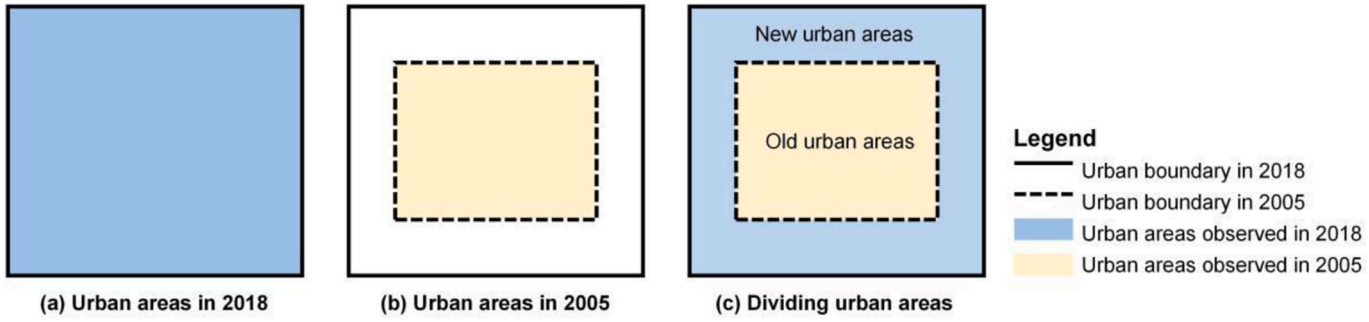

Fig. 2. The process of dividing urban areas.

assess global urban vitality from a social perspective, this study obtained 2020 population data worldwide from WorldPop (Tatem, 2017), which generates high-resolution open data on population distribution. The data were derived from a mosaiced global population dataset with a resolution of 1 km, using 100m resolution counts (Lloyd et al., 2019). By combining the global urban boundary data, the values of population density in old and new urban areas can be calculated. WorldPop's model is robust in identifying significant spatial relationships between census data and machine learning output, and excluding some rural population not found in built-up areas detected by satellite data (PopGrid Data Collaborative, 2020) to improve accuracy. The model is transparent with its methods and data sources, integrating a variety of data to redistribute population counts across census or administrative units (Stevens et al., 2015), and allowing global comparisons over time. As this study focuses on urban areas, WorldPop is suitable as the data source.

3. Results

3.1. Indicators between new and old urban areas indicate potential ghost cities in new urban areas

To gain a deeper understanding of the concept of ghost cities, it is crucial to first compare several key indicators between new and old urban areas (Fig. 3). According to the definition of ghost city, the ghost city index of a city depends on the difference of density of road network, density of POIs, and population density between new and old urban areas. Based on the standard of the United Nations (https://unstats.un.

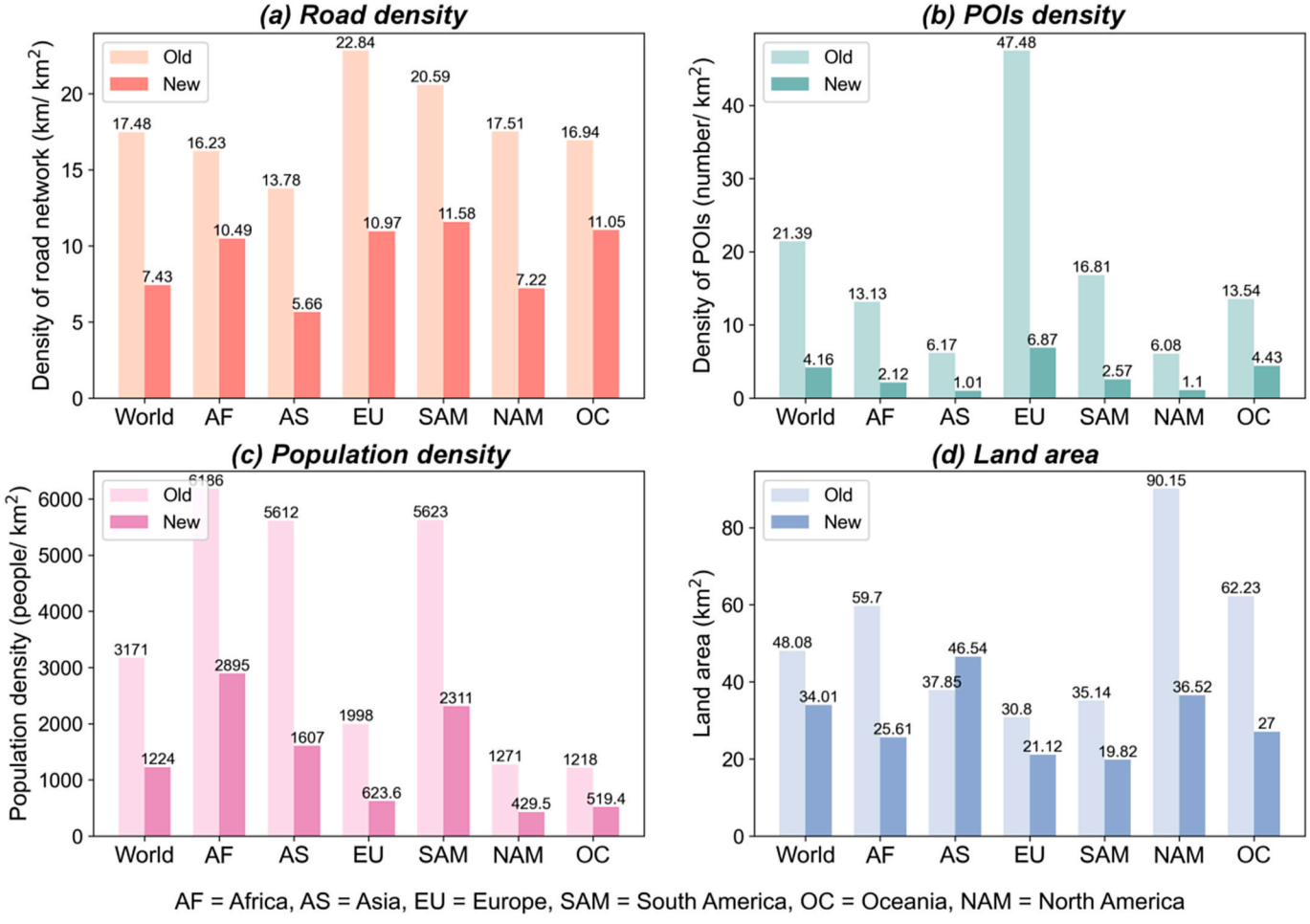

Fig. 3. Indicators of global new and old urban areas by geographic regions in average.

org/unsd/methodology/m49/), The geographic regions are divided into the continents.

Globally, new urban areas distinctly exhibit lower POIs density compared to old ones. However, the difference in population density is relatively modest, with the variance in road network density being the most minimal. In these new urban areas, the road network density constitutes 42.51%, the POIs density amounts to 19.45%, and the population density reaches 38.60%, when compared with those in older urban areas.

At the regional level, differences in road network density are generally minor, with Asia exhibiting the most substantial disparity. In this region, the road network density in new urban areas represents only 41.07% of that in older urban settings. A notable instance is China, where extensive real estate developments in newer urban districts have led to relatively less dense road networks. POIs density differences are striking, both between new and old urban areas and across regions. Asia and North America display lower average POIs densities, while Europe exhibits the highest. In regions excluding Oceania, new urban areas have a POIs density below 20% of older areas. Oceania, however, stands out with the smallest disparity, its comparative ratio being 32.72%. In terms of population density, the gap is most pronounced in Asia, where new urban areas account for just 28.63% of older areas. Conversely, Oceania showcases the least disparity, with a comparative ratio of 32.72%.

The results at the national level are shown in Fig. 4. In terms of density of road network, the differences between countries and their new and old urban areas tend to be much smaller than other indicators. Conversely, the variance in POIs density between new and old urban areas across countries is notably more significant. In this dimension,

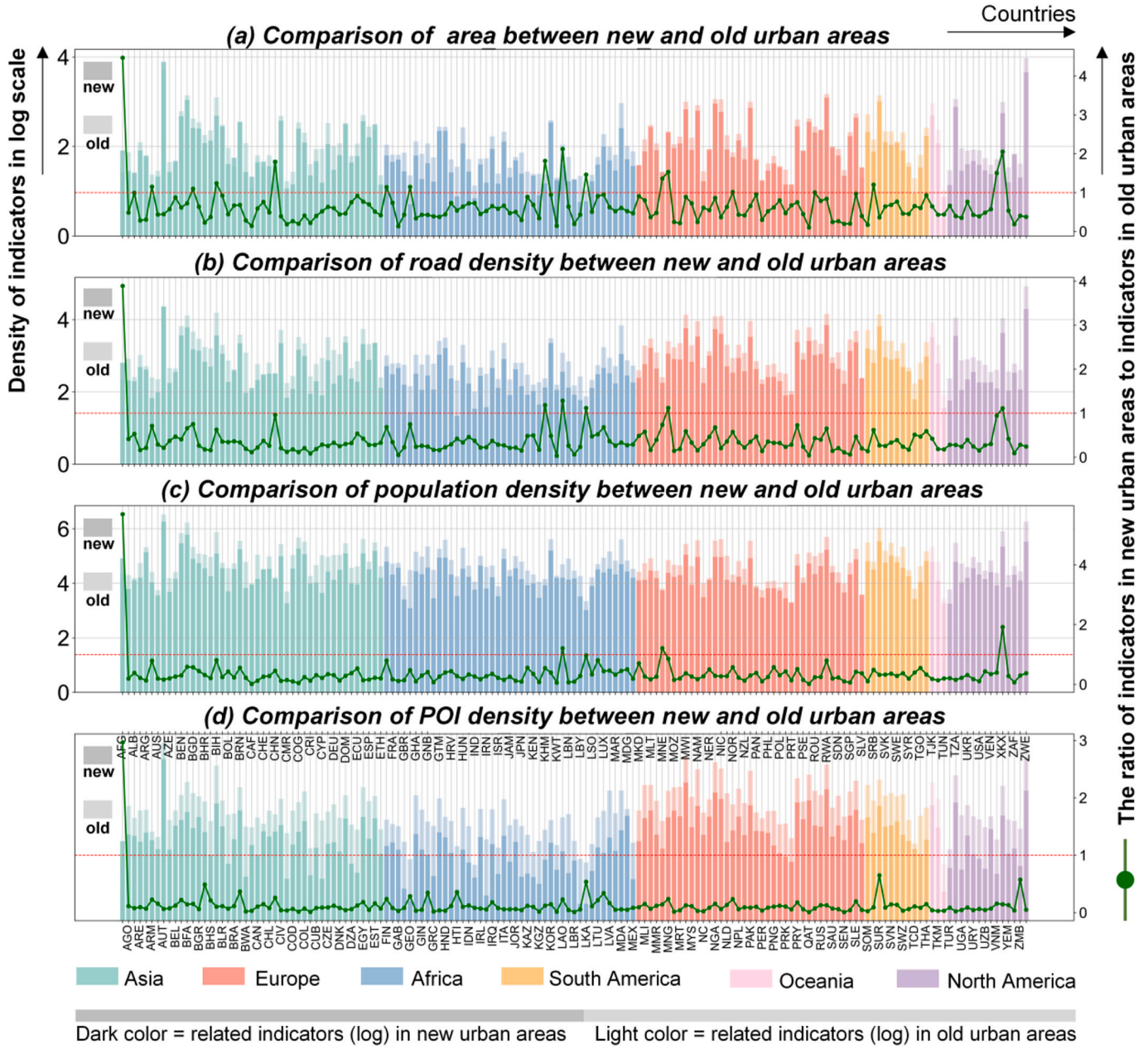

Fig. 4. Indicators for global ghost cities at the national average level. Each bar represents a country, and different colors indicate different regions. "old_area", "new_area", "roads_old", "roads_new", "old_pop_num", "new_pop_num", "poi_old", "poi_new" represent the density of each indicators in new and old urban areas. All the real indicator values on the left are scaled by log 20 to facilitate visualization, and the ratio on the right is the real index values of the indicators in new urban areas to old urban areas. The last sub-picture gives the abbreviations of all countries (Supplementary Table 7). (For interpretation of the references to color in this figure legend, the reader is referred to the Web version of this article.)

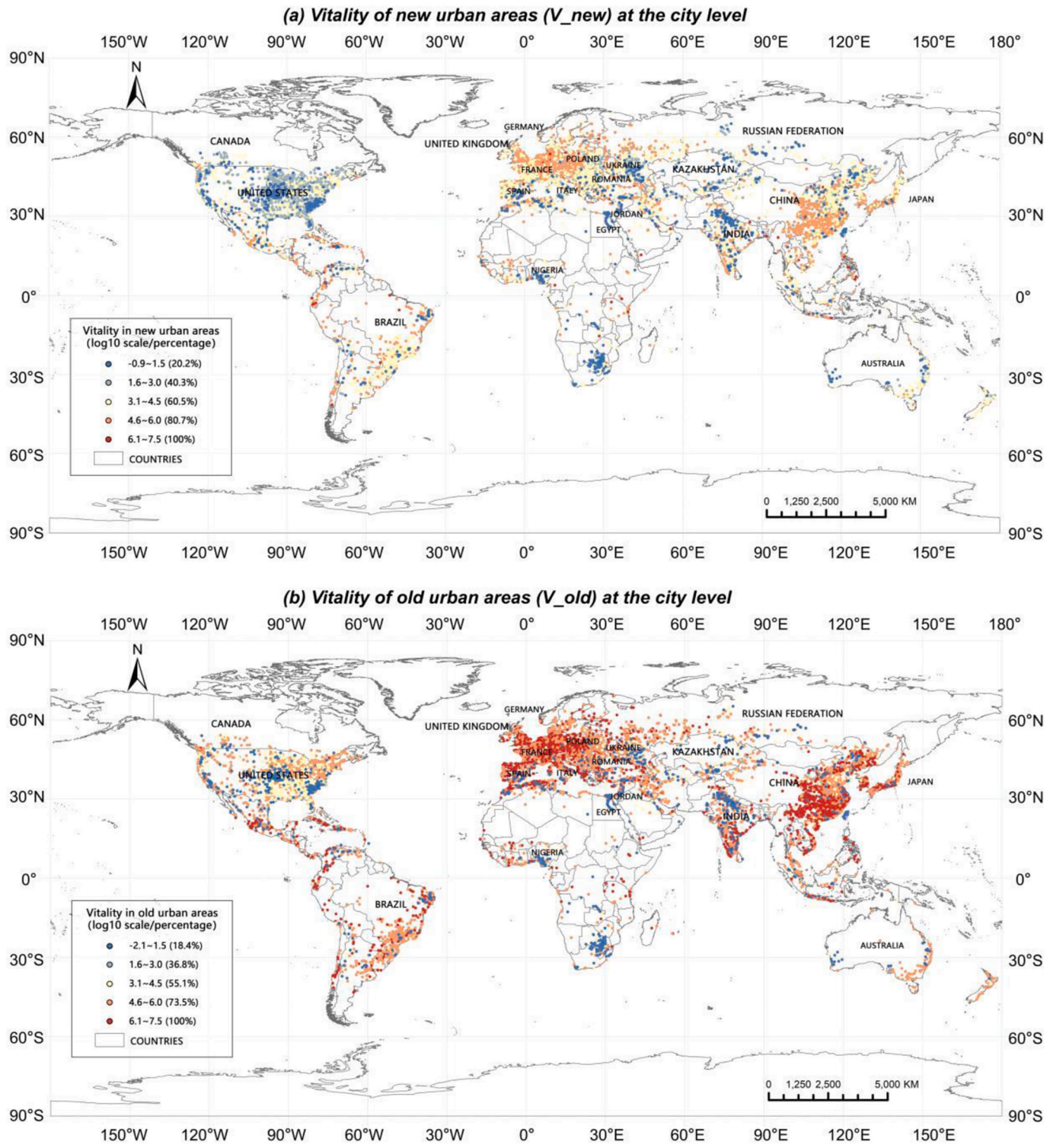

Fig. 5. The vitality of new and old urban areas for cities on the globe. Each point represents a natural city. All the real index values on the left are scaled by log 10 to facilitate visualization. The ratio on the right side of the legend refers to the number of existing cities up to the interval to the total number of cities.

most African countries exhibit lower levels, whereas many European countries demonstrate significantly higher levels. Regarding population density, a reverse trend is observed, with many European countries showing lower levels compared to African countries. The difference of the land area between new and old urban areas is relatively small for most countries, which is similar to density of road network (see Fig. 5).

3.2. The vitality of global urban areas at different level

To investigate the characteristics of global urban vitality, this study compares the vitality values of old and new urban areas at various levels, including city, national, regional, and global scales. Initially, the study examines the distribution patterns of urban vitality at the city level. Cities with higher vitality are mainly concentrated in Europe, East Asia, and South America as well as some tropical regions (Fig. 3). Although

the distribution patterns of vitality are broadly similar between new and old urban areas, it is notable that new urban areas tend to have fewer high vitality points compared to old urban areas. In more developed nations, such as the United States, the vitality differential between new and old urban areas is less pronounced than in developing nations, notably India and China. The vitality of new and old urban areas in Europe displays notable differences, suggesting a distinct development model from other developed countries, as indicated by the 'ghost city index' (Fig. 7).

Then the study analyzed the vitality of global urban areas at national, regional and global level (Fig. 6). For each level, we recalculated indicators to obtain average vitality values for old and new urban areas. Most new urban areas have vitality accounting for less than 10% of their older counterparts at both national and regional levels. Globally, the vitality of new urban areas is just 7.69% of that in older areas. This significant disparity underscores the low vitality in newer regions. While it is evident that new urban areas generally exhibit much lower vitality than older ones, these findings reinforce the notion that assessing the vitality difference between new and old urban areas is an effective approach to identify the ghost cities on the globe.

3.3. Visualization of ghost city index on the globe at city level

Fig. 7 maps each city's Ghost City Index (GCI). Cities with elevated GCI values are particularly prevalent in East and South Europe, Northeast China, and certain regions of the United States, underlining the

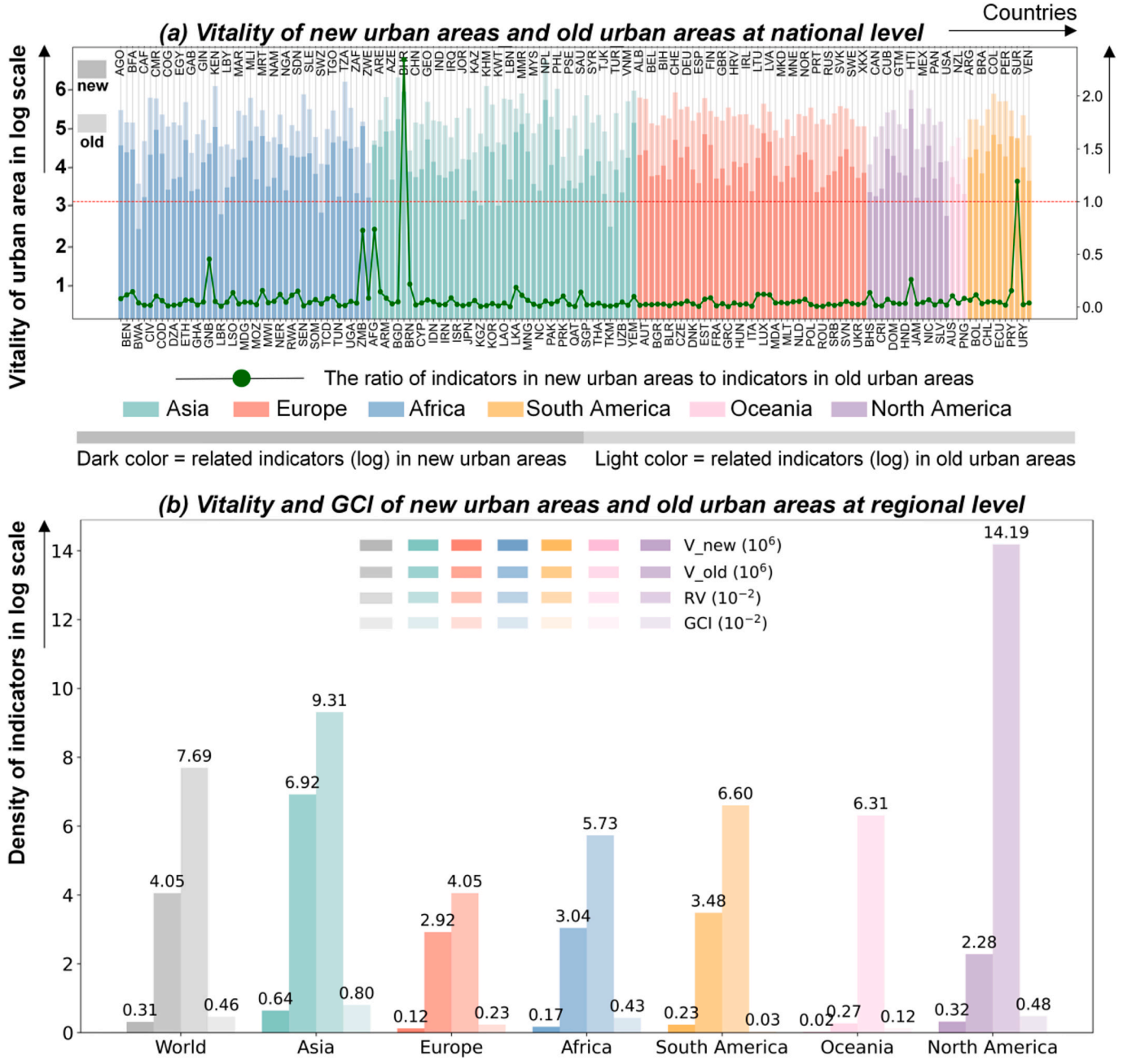

Fig. 6. Vitality of new urban areas and old urban areas at the national and regional level. (a)Each bar represents a country, and different colors indicate different regions. All the real index values on the left are scaled by log 20 to facilitate visualization, and the ratio on the right means the real vitality index in new urban areas to that in old urban ares at national scale. (b)RV=Ratio of vitality between new and old urban areas. (For interpretation of the references to color in this figure legend, the reader is referred to the Web version of this article.)

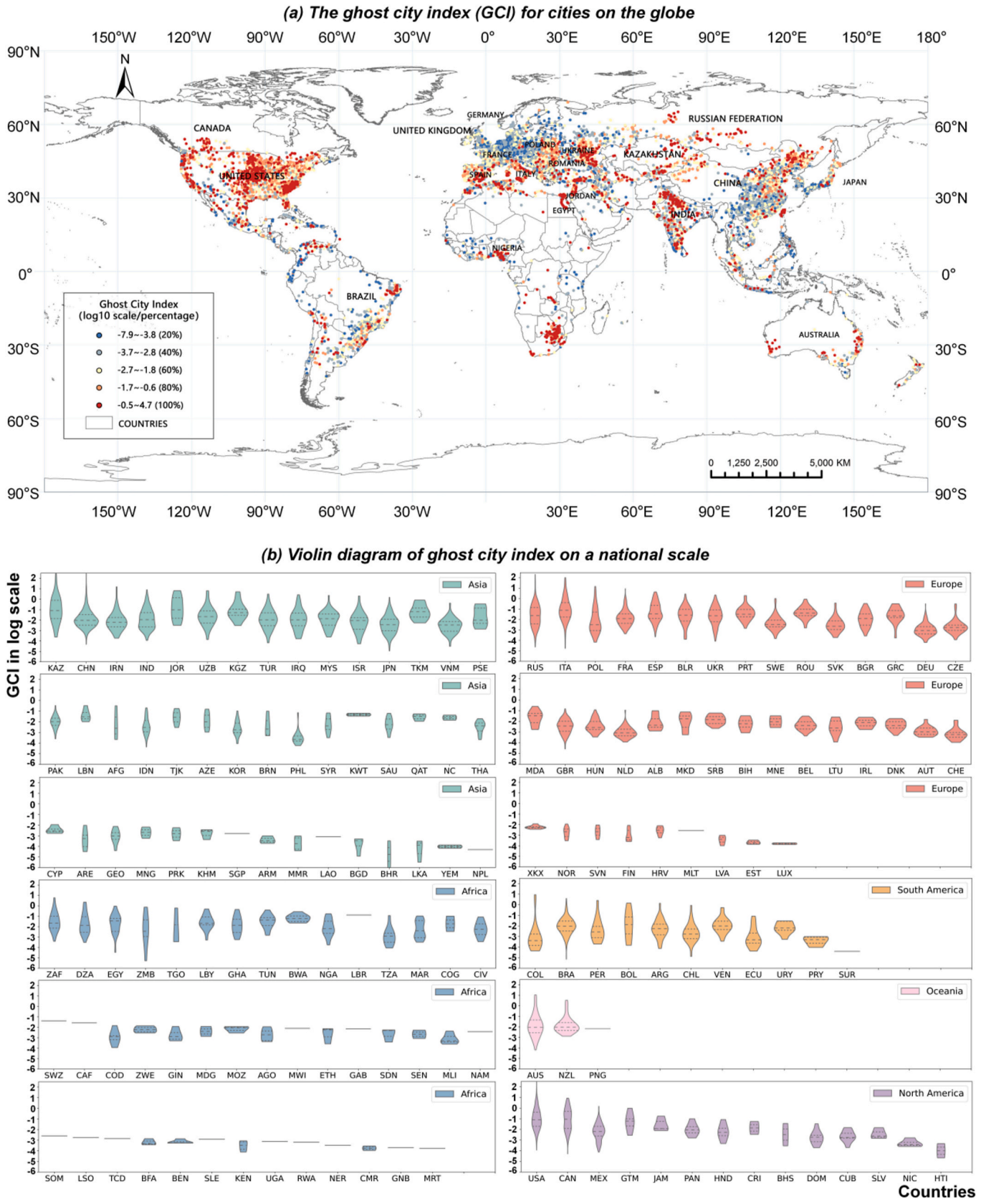

Fig. 7. The ghost city index (GCI) for cities and countries on **the globe.** (b) Violin diagram shows the distribution shape, median, and quartile distribution of ghost city index (GCI) calculated by each country. GCI are scaled by log 20 to facilitate visualization.

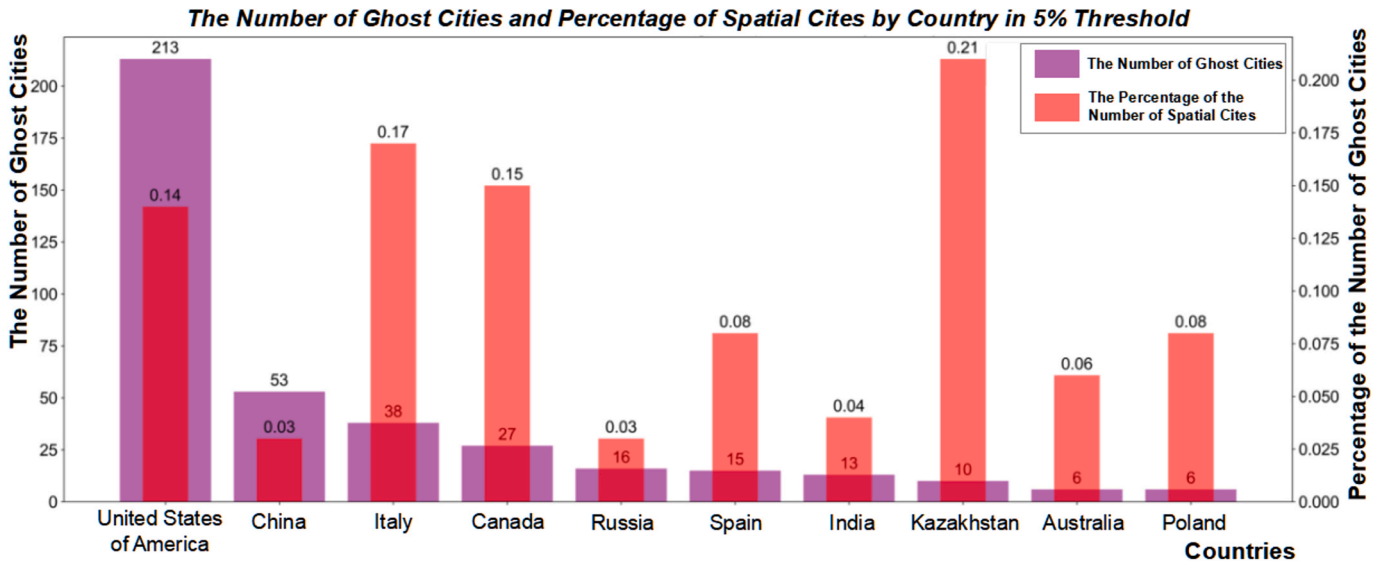

Fig. 8. Selection of ghost city threshold and the top ten countries with the largest number of ghost cities.

global scope of the ghost city challenge. In a broader view, United States of America has a notable number of ghost cities, whereas Asia presents fewer. Meanwhile, Europe and Africa have relatively high counts and proportions of such cities.

Interestingly, some cities, while exhibiting high vitality in absolute terms, also maintain elevated GCI values. This indicates a marked disparity in vitality between new and old urban sectors (Fig. 7). For instance, while cities in Europe and Asia demonstrate high vitality, the GCI in Northern Europe is significantly lower than in East and South Asia. A closer look at Fig. 7(b) reveals a near-normal distribution of GCI values across cities in Asia and Europe. In contrast, a majority of African cities possess a lower GCI, indicating a state of imbalanced urban development.

3.4. Inferring ghost cities' distribution on the globe

The ranking of GCI values of global natural cities was utilized to infer the distribution of ghost cities, examining the number of cities and countries beneath various GCI thresholds, the proportion of identified ghost cities in all natural cities within each country, and ultimately setting the top 5% (442 out of 8841 natural cities) as a threshold (see Fig. 6) for visualization. The specific rankings can be accessed in the attached Supplementary Tables. We then focused on the top ten countries with the highest number of ghost cities, as depicted in Fig. 6. Notably, the United States, China, and Italy lead this list, having the most significant count of ghost cities within their new urban areas. When comparing the proportion of ghost cities to the total number of natural cities within a country, Kazakhstan, Italy, Canada, and the United States stand out, as showcased in Fig. 6.

To illustrate our findings, we focus on the distribution of ghost cities in these countries (Fig. 9). Consistent with existing research, our findings also spotlight the United States and China as key regions of interest in the ghost city phenomenon. In the United States, ghost cities predominantly feature in the Midwest and eastern coastal areas. In contrast, China's ghost cities are primarily clustered in its northeast and northern regions. Overall, these findings suggest that while the phenomenon of ghost cities is present in multiple countries. However, the intensity and underlying reasons for these ghost cities differ across nations.

3.5. Benchmarking our results from news media and related research

To validate the inferred ghost cities in new urban areas, we compared our calculation results with news media and existing related rankings. First of all, we directly combine 'ghost city' with the names of all cities in the world (data comes from GADM), search on Google, and rank the number of search results of each city as the measure of the public's perception and media interest of ghost cities. Table 2 ranks the top 20 countries with the largest proportion of search result cities at different segments (Top 5%–25% cities) in ranked Google search results. We can find that they are highly consistent with the ghost cities identified by GCI at the national level (Fig. 8), such as the United States, Canada, Italy, and Russia. They exist in different segments, and the high ranking of the United States' search index further verifies the results of GCI. Overall, the search result indicates that our identification results for ghost cities align with the general perception of such cities worldwide.

While several studies have depicted ghost cities using data such as population and night-time light, no one has quantitatively ranked the global ghost cities index according to our investigation, making it difficult to compare the rationality of our index with previous research on a global scale. To address this, we benchmarked our results with empirical research and news media at different regional scales, such as the Biaozhun ranking, Shi et al. (2020), Pradamini Kumari (2019) and Chuah, P. L.'s research (2020), focusing on China and the United States (Supplementary Table 6). In terms of ghost cities in China, the Biaozhun ranking and the research of Shi et al. (2020) have some similarities compared with our results. We all agree that top ghost cities are mainly distributed in the northeast and northern China, including some cities like Wuzhong (Ningxia), Aletai (Xinjiang), Yichun (Xinjiang), Weihai (Shangdong) and Qitaihe (Heilongjiang). As for ghost cities in the United States, the news reports of Pradamini Kumari (2019) and the 24/7 Wall St Ranking show many ghost cities in the United States consistent with our research results, both tending to locate ghost cities in the middle and northern regions of United States. However the news media and related research are more concerned about the vacancy of houses, so their results have limitations in application.

3.6. Understanding the distribution of GCI from different perspective

Based on the derived 8841 natural cities, we calculated the population change and land expansion through the WorldPop data, and understood the global distribution of GCI from the perspective of population change (Fig. 10). Firstly, a total of 1825 natural cities have experienced population shrinkage and 7016 natural cities have experienced population expansion. Secondly, Fig. 8 indicates that population growth and land expansion are often concentrated in large cities, especially in North America and Asia, showing the highest urban expansion

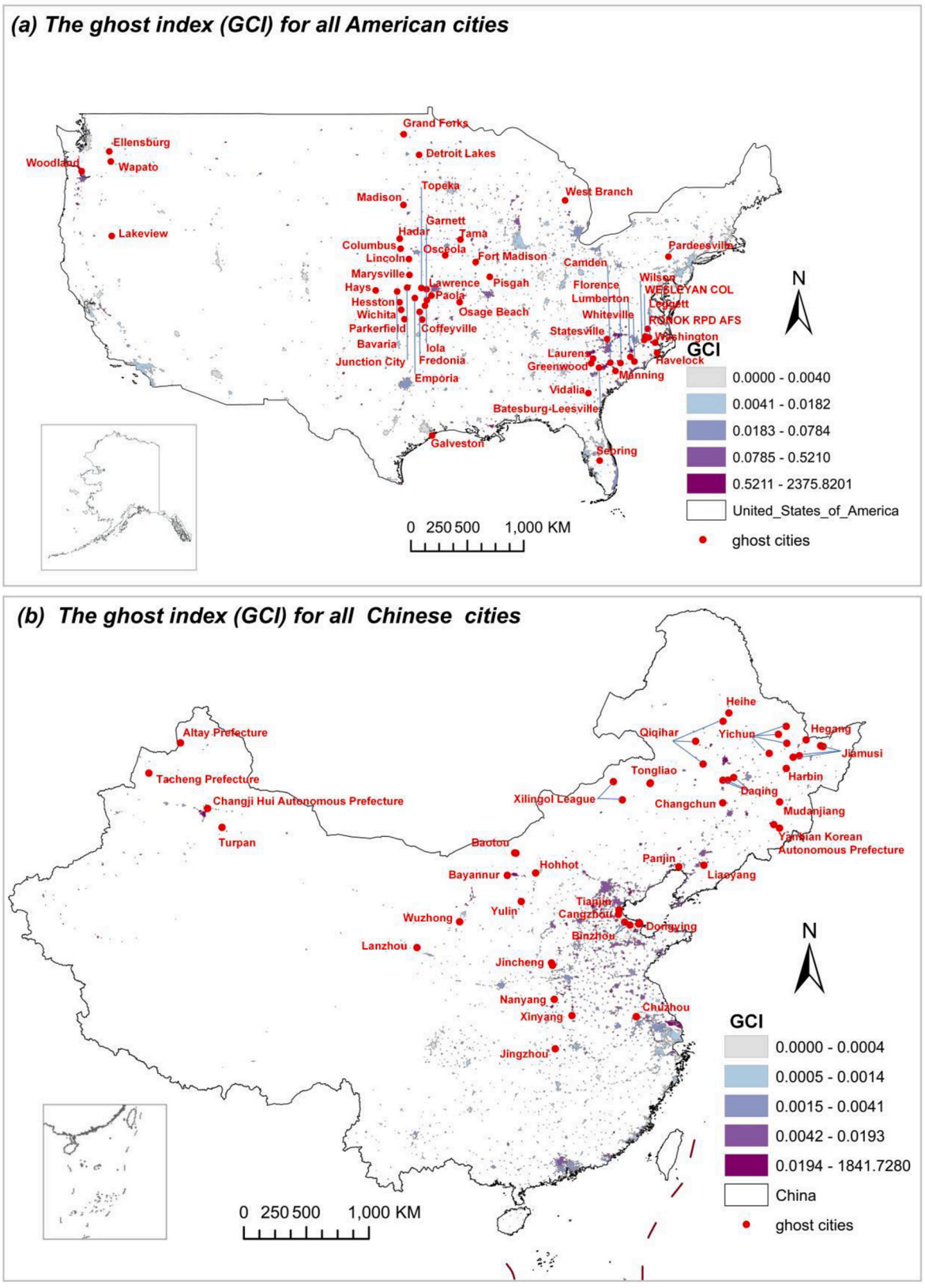

Fig. 9. The ghost index (GCI) for the top ten countries with the largest number of ghost cities and a zoomed-in map for identified gho**st cities.** (a), (b), (c), (d), (e), (f), (g), (h), (I), and (j) respectively reveal the ghost city index of each country and the visualization of ghost cities under the specified threshold, in which the United States only shows the top 50 ghost cities, and Canada's visualization omits the areas without ghost cities because of its large land area.

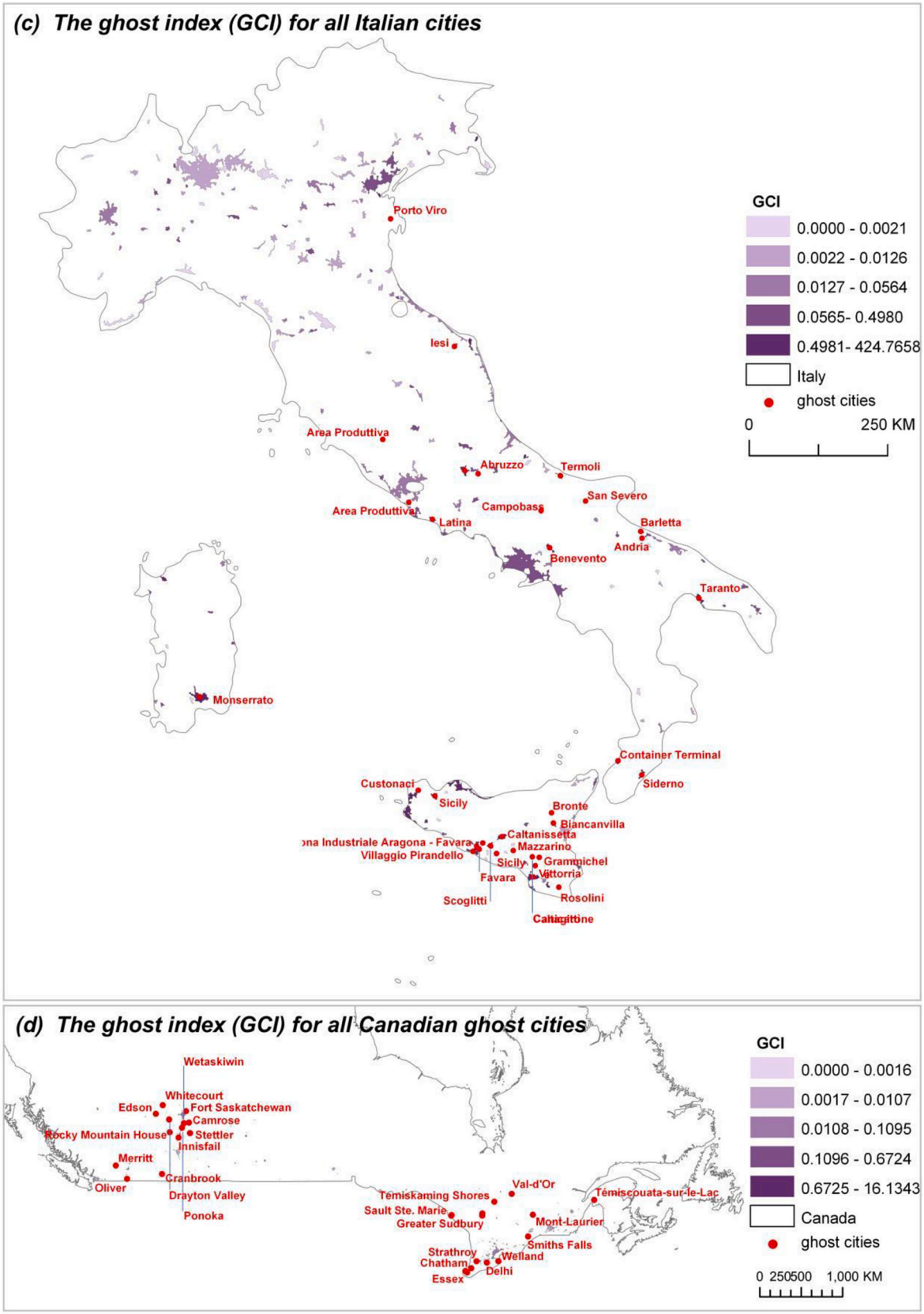

Fig. 9. (*continued*).

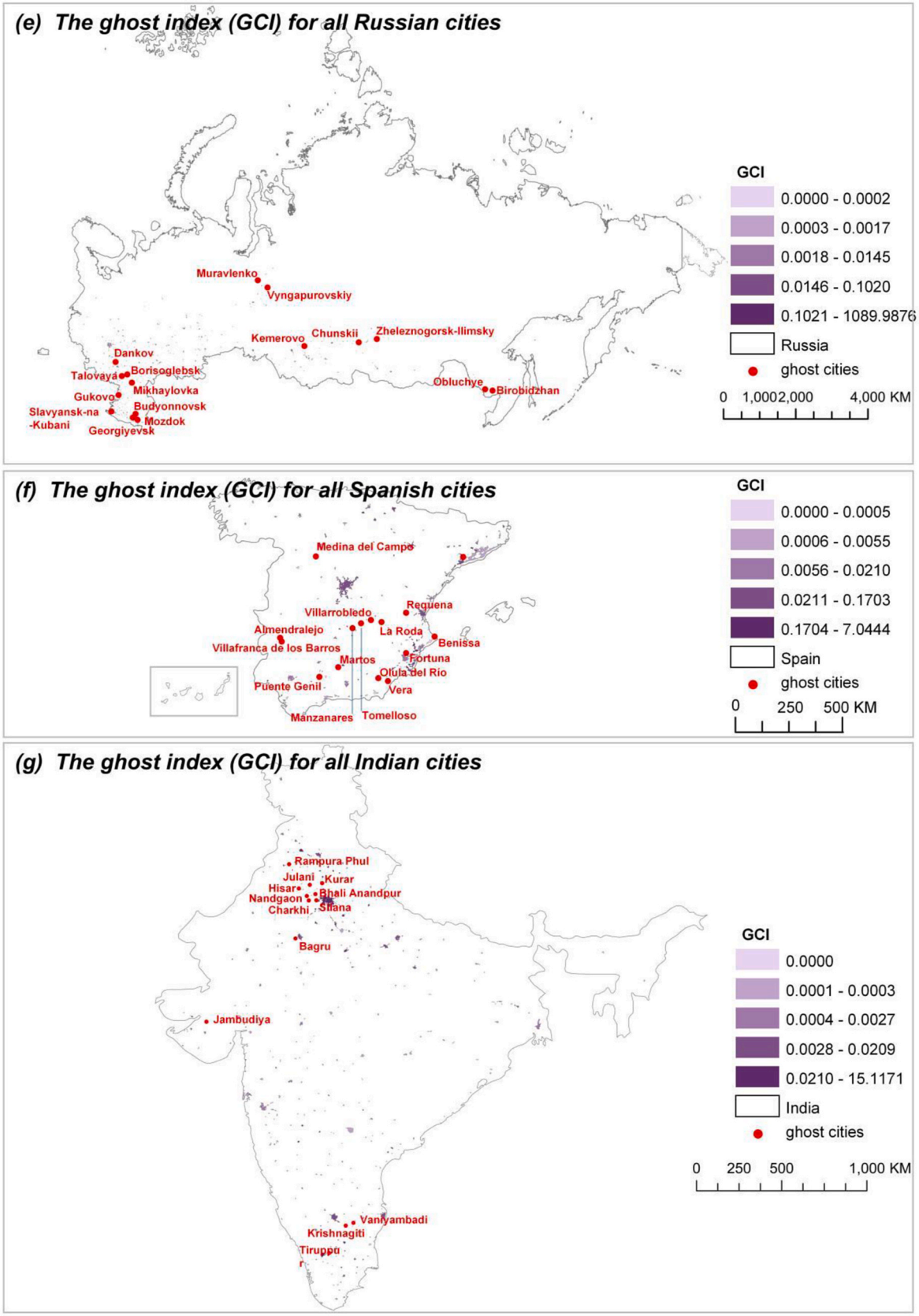

Fig. 9. (*continued*).

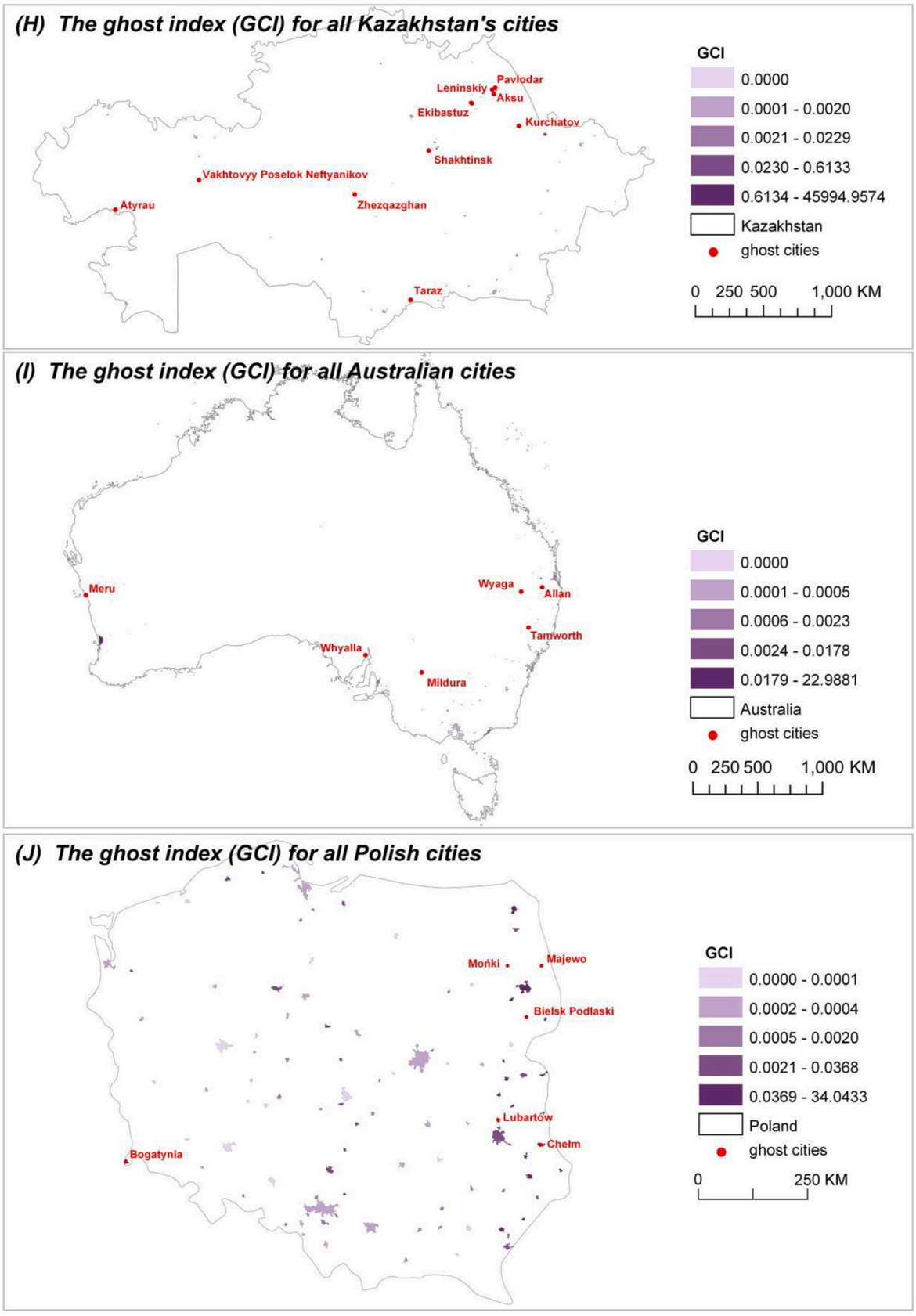

Fig. 9. (*continued*).

Table 2
Top 20 countries with the most ghost cities in Google search results.[a].

Rank	Top 5%[b]		Top 10%		Top 15%		Top 20%		Top 25%	
1	*[c]United States	0.346	*United States	0.250	Philippines	0.008	Philippines	0.235	Philippines	0.248
2	*Canada	0.222	Philippines	0.177	*United States	0.006	*United States	0.147	*United States	0.120
3	Philippines	0.132	*Canada	0.161	*Canada	0.005	*Canada	0.129	*Canada	0.120
4	Germany	0.084	Germany	0.110	Germany	0.005	Germany	0.100	Germany	0.096
5	United Kingdom	0.036	*Italy	0.058	*Italy	0.003	*Italy	0.085	*Italy	0.096
6	Portugal	0.025	Portugal	0.029	Portugal	0.003	Thailand	0.040	Thailand	0.043
7	*Russia	0.024	United Kingdom	0.029	Thailand	0.003	Portugal	0.039	Portugal	0.042
8	Thailand	0.022	Thailand	0.026	United Kingdom	0.003	*India	0.019	*India	0.021
9	*Italy	0.016	*Spain	0.015	*India	0.003	Switzerland	0.017	Indonesia	0.018
10	*Austria	0.008	*India	0.014	Estonia	0.002	United Kingdom	0.017	Switzerland	0.017
11	*India	0.008	*Russia	0.013	Switzerland	0.002	Estonia	0.016	Estonia	0.014
12	Peru	0.008	Switzerland	0.013	*Spain	0.002	Indonesia	0.013	United Kingdom	0.014
13	Estonia	0.008	Estonia	0.012	*Russia	0.002	*Poland	0.013	*Poland	0.013
14	Panama	0.007	*Austria	0.011	Peru	0.002	Peru	0.012	Peru	0.012
15	Switzerland	0.007	Peru	0.010	*Austria	0.001	*Spain	0.011	*Austria	0.010
16	Chile	0.005	Costa Rica	0.008	*Poland	0.001	*Austria	0.011	*Spain	0.010
17	Ecuador	0.005	France	0.007	Indonesia	0.001	*Russia	0.010	*Russia	0.009
18	*Spain	0.004	*Poland	0.006	Costa Rica	0.001	Costa Rica	0.009	Ecuador	0.009
19	*France	0.004	Panama	0.005	France	0.001	Ecuador	0.008	Costa Rica	0.008
20	*Poland	0.004	Chile	0.005	Ecuador	0.001	France	0.007	*China	0.008

c*represents the country in the 20 countries in this percentage grading that coincide with the countries in Fig. 6.

[a] In order to keep the global unified administrative boundary division and acquire all of cities' names, we use the multilevel administrative boundary data from the Database of Global Administrative Areas (GADM, https://gadm.org/), and adopt level 3 as the retrieval combination mode (province/state + major cities + towns + ghost city/town). The ranking of ghost cities adopted by this study is the smallest division from the location of natural cities among the three-level administrative divisions in the world.

[b] Different segmentation, such as 5%, means that the top 5% of all cities in Google search results are used as the threshold of ghost cities, and then the countries to which these cities belong are counted and ranked according to the proportion of ghost cities owned by countries to all natural cities in the country.

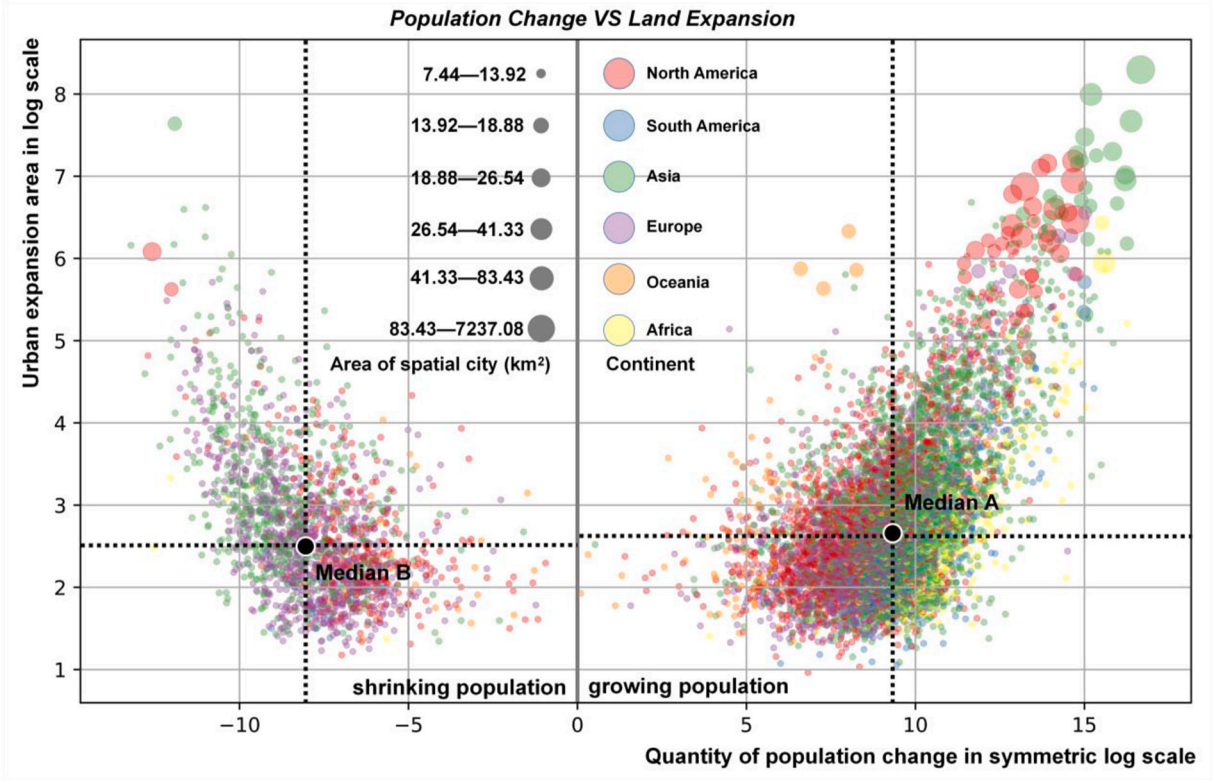

Fig. 10. Relationship between population change and land expansion in all the 8841 natural cities around the world. The vertical axis at the zero point of the horizontal axis represents the relationship between population change and land use expansion under the two conditions respectively. Median A and B represent the specific values of the median city of population expansion (contraction) and the median city of land expansion respectively. In order to facilitate visualization, symmetric logarithmic transformation is used for population change data and logarithmic transformation is used for land expansion data.

speed. At the same time, compared with other regions, the population growth rate in South America and Africa is higher than the land expansion rate. Population growth faster than land expansion will lead to a high vitality index of new cities, which can also explain why the ghost city index in these areas is relatively low. On the contrary, the population expansion rate of a large number of North American cities is relatively low compared with the land expansion rate, which accounts for the existence of a large number of ghost cities in new urban areas in the United States.

3.7. Is it reasonable to identify ghost cities by nighttime light data?

As a complement to utilizing micro-level data (including road networks, population and POIs) for identifying ghost cities, we reference Jin et al. (Jin et al., 2017), who employed the DMSP nighttime light data (NTL) for validation. Advances in sensor technology have mitigated the saturation effects inherent in the VIIRS series compared to DMSP, thereby enhancing the capability to distinguish highly illuminated urban areas more effectively. As illustrated in Supplementary Fig. 3(b), the DMSP series data, even after synthetic processing to extend beyond 2012, exhibits pronounced saturation effects, whereas the VIIRS series data does not. We analyzed multi-year night-time light imagery to compute the average Digital Number (DN) values of pixels within newly developed urban areas (post-2005) and pre-existing urban areas (as of 2005) for each city across China. These averaged DN values for both urban area types are depicted in Supplementary Fig. 3(a). A significant disparity is observed between new and old urban areas, with most cities displaying substantially lower illumination levels in new urban areas compared to old ones, irrespective of the time period. Aligned with urbanization trends, the gap in nighttime light between new and old urban areas has progressively narrowed from 2012 to 2021.

However, due to resolution limitations, NTL is less suitable for directly identifying ghost cities compared to finer-grained data such as POIs, road networks, and population data. Nevertheless, it can serve as a reference for characterizing urban vitality at a macro level. The reasons why NTL is not suitable for directly identifying ghost cities are as follows: First, the spatial resolution of NTL is 1 km, which is insufficient to capture small-scale urban vitality changes compared to vector-based POIs and road data. Second, brightly lit streets at night do not guarantee the full utilization of other indicators reflecting urban vitality in newly developed urban areas, as the development of road infrastructure (e.g., wide streets and bright lighting) often precedes housing development (e.g., locations of POIs and population agglomeration). Supplementary Fig. 4 demonstrates that in a few cities (especially in China (Jin et al., 2017)), new urban areas tend to have higher lighting levels at lower road densities compared to old urban areas, indicating that bright nighttime lights are not always associated with urban vitality.

Despite these limitations, NTL shows significant potential in validating the urban vitality and ghost city index measurement framework proposed in this study, for the following reasons: First, Supplementary Fig. 3 shows that most cities exhibit significantly lower lighting levels in new urban areas and can reflect the temporal dynamics of urban development. Second, the VIIRS series, compared to the previously used DMSP data (Jin et al., 2017), has reduced saturation effects and better distinguishes differences between new and old urban areas (see Supplementary Fig. 3). With advancements in nighttime light satellite technology, the feasibility of using increasingly higher-resolution NTL data to capture urban vitality will continue to improve. Finally, until the availability of global data (e.g., social media data and human commuting data) improves, NTL remains the only openly accessible datasets capable of characterizing urban vitality at a global scale. Existing data such as GDP and electricity consumption are often mapped using NTL and allocated top-down to each city based on national statistical indicators, yielding regression results similar to those of NTL (see Supplementary Fig. 4) (Chen, Gao, et al., 2022).

3.8. Choice of the time division for dividing new and old urban areas

In this study, 2005 was uniformly chosen as the cutoff for distinguishing between new and old urban areas. However, we acknowledge that this approach does not fully capture the varying development stages of new urban areas. The vitality of these areas may differ significantly depending on whether they are in the construction, development, or maturity phase, with each stage presenting distinct manifestations of the ghost city phenomenon and its underlying causes. For instance, new urban areas in the early stages may exhibit high vacancy rates due to overdevelopment or poor planning, yet retain growth potential. In contrast, ghost cities in the decline phase may experience low vitality due to functional decay and commercial inactivity.

Due to the differences in the development stages of various cities, the rationale for using the same time point to distinguish between new and old urban areas needs to be confirmed. First, we used boundary data from every five years between 1990 and 2015 (GUB1990-2015). We calculated the changes in the total urban area of the world and individual countries (visualization only retained countries with urban areas larger than 10,000 square kilometers, as shown in Supplementary Fig. 7). It can be observed that from 2005 to the present, the global urban area has increased by nearly half, and choosing this time point helps in comparing and analyzing data within the range of new and old cities, reducing errors caused by differences in scale.

Second, we classified global cities into four categories based on urban area and average Per capita GDP to represent different development levels. Then, we analyzed the differences in the “Ghost City Index” (GCI) for each category (see GCI_BF in Supplementary Fig. 6). We found that cities at different levels of development indeed exhibit different GCI distribution patterns. Cities with large sizes and low Per capita GDP are more likely to have high GCI, possibly due to rapid growth in such cities, where the difference between new and old urban areas is too large. This is commonly seen in developing countries like China and developed countries like the United States. Cities with high GCI relatively small sizes, and low Per capita GDP are more common in developing countries in Africa. Cities that are small in size but have high Per capita GDP are mostly located in European countries. These cities have more balanced spatial development and a lower GCI.

Future research should therefore provide a more nuanced analysis of ghost cities, considering their development stages and underlying causes, such as disaster-related, decayed, or planning-induced ghost cities. This will allow for a more comprehensive understanding of the ghost city phenomenon and its internal dynamics. Meanwhile, considering the high complexity of long-term global computations involving road and POIs data, future studies may leverage nighttime light data to explore the urban life cycles within individual countries or regions.

4. Discussion and conclusion

This paper presents a bottom-up method by utilizing publicly available open-access data to investigate the phenomenon of ghost cities in new urban areas across all natural cities worldwide. We claim that the conceptualization of a “ghost city” is characterized by the presence of expansive urban form, undeveloped urban functions, and very sparse human mobility/activity density (Jin et al., 2017). For the first time, we attempt to rank ghost cities on the globe and provide an overall identification and verification of cities on the globe at different scales.

In the results of identifying ghost cities, we not only verify the known facts, such as the distribution of ghost cities confirmed by previous studies on local scales but also summarize the differences in the development of new urban areas in different countries and regions. First, countries and regions in different urbanization stages have different characteristics of urban vitality and ghost cities. Although the results confirmed again that new urban areas have a lower vitality level than old urban areas, however, the difference in the ghost city index among Africa, Asia, and Europe shows the different urbanization stages of these

regions. At the stage of vast urban expansion in Asia, many new urban areas are built up without enough infrastructure, facilities, and population, resulting in a higher ghost city index. At the later period of urbanization like in some European countries, especially in western and northern Europe, the contrary is the case.

Second, for all the cities worldwide, we can find that the high ghost city index mainly comes from the lack of the functional dimension of the new urban areas. The road density usually shows a small gap compared with other indicators in the new and old urban areas, which is easy to understand, because the expansion of urban built-up areas is often ahead of the migration of population and the supplement of facilities policies, especially in some developing countries. At the same time, the difference in activity density is similar to the road density at the global level, far less than the difference in functional infrastructure. However, at the regional level, it can be found that there are great differences in the development of new urban areas in different countries and regions. The high index of Asian ghost cities is the joint result of the interaction of three dimensions, which probably comes from the fact that compared with other regions, Asian cities have the fastest expansion. Africa, which is also a gathering place of developing countries, shows different characteristics from Asia in the ghost city index, and more comes from population activities and functional infrastructure.

Third, the findings of this paper highlight the widespread distribution of ghost cities as a severe global problem, particularly in North America, Asia, and parts of Europe. The results of our identification on a global scale show that the distribution of ghost cities is concentrated in the United States, China, Italy, and other major countries. Unlike what we expected, the United States, as a developed country, has a large number of ghost cities, compared with other countries. On the one hand, we speculate that many developed countries have been affected by the cyclical economic crisis, and some so-called ghost cities may be related to the long-term impact of the 2008 crisis, especially in the United States. Although China does not have a high proportion of ghost cities, due to rapid urbanization, it still has many ghost cities. On the local scale, our ghost cities are located in the northeast of China and the east coast of the United States, which is consistent with the previous research findings and news media(Jin et al., 2017; Shi et al., 2020). This reveals the significance of spatial planning and development strategies in coping with ghost cities and building sustainable cities. Our validation results prove the rationality of this method, in which the search rankings for Chinese ghost cities are notably lower across the segments. This could be attributed to the limited popularity of Google searches in China.

According to the results, policy implications can be provided in the following aspects. First, since the high ghost city index is mainly caused by the functional dimension of new urban areas at the global scale, functions in new urban areas of many developing countries need significant improvement. The lower density of POIs reflects fewer functions, including amenities, public services, and jobs. More functions can be the key to mitigating ghost cities on the global scale. Second, the policy-making of urbanization strategies should consider the urbanization stage. For low-income countries like some African countries, it could be better to make an evaluation of the development situation in old urban areas and keep a proper construction size of new urban areas, Third, spatial planning in new urban areas should consider proper population density and optimize land use configuration, especially the developing countries in Aisa. Denser roads should be taken into account to improve spatial accessibility and urban vitality.

This study employs a comparative analysis of new and old urban areas to identify urban vitality and calculate the GCI, a metric reflecting intra-city developmental imbalances. While the GCI enables cross-city comparisons, the methodology faces limitations due to data incompleteness and the relative nature of such comparisons. Urban vitality indicators—road network density, population density, and POIs density—are grounded in Jacobs' classic theory, yet empirical support for this framework remains scarce, particularly in diverse global contexts. Existing studies (e.g., Huang, 2023) are limited in number (only five) and exhibit inconsistent quantitative results, raising concerns about the robustness and cross-regional applicability of the theory. Moreover, there is no consensus on the specific indicators contributing to urban vitality, necessitating careful selection and validation of metrics. Due to data constraints, this study simplifies Jacobs' framework into three dimensions, with nighttime light data used to preliminarily assess their sufficiency and necessity. Localized GCI validation was also conducted using search engine data and existing studies.

The GCI's interpretation requires attention to contextual factors. Seasonal population fluctuations, such as in tourism-dependent cities, or the prolonged effects of economic disruptions (e.g., the 2008 financial crisis), may temporarily depress vitality, leading to elevated GCI values that do not reflect long-term trends. Smaller cities, with lower thresholds for residential development, may also exhibit higher GCI values due to scale rather than significant declines in vitality. Additionally, new urban districts in early development phases may show temporarily low vitality, which should not be conflated with long-term "ghost city" characteristics. These nuances highlight the importance of contextualizing GCI results within socio-economic and developmental frameworks. Future research could refine the methodology by incorporating such adjustments, enhancing its precision and applicability across diverse urban settings.

This study shows that identifying ghost cities on the globe and their spatial differences is of great significance for understanding the urbanization process and building a sustainable city. Some local scale studies have discussed the definition and recognition of ghost cities, but they have not yet formed a globally recognized recognition framework. Nevertheless, we believe that our bottom-up approach is a straightforward and sustainable framework for evaluating ghost cities. Different from the recent research, we pay more attention to the comparability and easy use of the identification of ghost cities in the world. By dividing the boundaries of natural cities based on the time series and using publicly available open-access data, we overcome the limitation that previous studies can only focus on the identification of ghost cities on a certain local scale. This comparison based on its urban spatial development shows the advantages of crossing geographical spatial heterogeneity. Future research should delve deeper into the causes, stages, and critical values of the ghost city phenomenon. Additionally, given the data limitations like OSM at the global level, the analysis is expected to be further deepened with the data environment continues to evolve (Zhang et al., 2024).

CRediT authorship contribution statement

Yecheng Zhang: Writing – original draft, Visualization, Validation, Software, Investigation, Methodology, Writing – review & editing. **Tangqi Tu:** Writing – original draft, Investigation, Formal analysis, Resources, Software. **Ying Long:** Supervision, Project administration, Funding acquisition, Conceptualization, Resources, Writing – review & editing.

Data availability

All reference data come from open databases, and their download channels have been shown in the method section (refer to Table 2). The primary datasets and codes of this paper have been uploaded to "Mendeley Data, doi: 10.17632/ypj9s32tn6", which describes all the data generated in this paper. This includes the spatial location of 8842 natural cities calculated in this paper, the attributes of new and old urban areas and the ghost city index.

Funding sources

This work was supported by the National Natural Science Foundation of China [Grant No. 62394331], [Grant No. 62394335] and [Grant No. 52178044].

Declaration of competing interest

The authors declare that they have no known competing financial interests or personal relationships that could have appeared to influence the work reported in this paper.

Acknowledgements

Thanks to Master Qingxiang Meng for his contributions to the original data calculation.

Appendix A. Supplementary data

Supplementary data to this article can be found online at https://doi.org/10.1016/j.habitatint.2025.103350.

References

Akinci, Z. S., Marquet, O., Delclòs-Alió, X., & Miralles-Guasch, C. (2022). Urban vitality and seniors' outdoor rest time in Barcelona. *Journal of Transport Geography, 98*, Article 103241.

Aubrecht, C., Gunasekera, R., Ungar, J., & Ishizawa, O. (2016). Consistent yet adaptive global geospatial identification of urban–rural patterns: The iURBAN model. *Remote Sensing of Environment, 187*, 230–240.

Barrington-Leigh, C., & Millard-Ball, A. (2017). The world's user-generated road map is more than 80% complete. *PLoS One, 12*, Article e0180698.

Batty, M. (2016). Empty buildings, shrinking cities and ghost towns. *Environment and Planning B: Planning and Design, 43*, 3–6.

Biljecki, F., Chow, Y. S., & Lee, K. (2023). Quality of crowdsourced geospatial building information: A global assessment of OpenStreetMap attributes. *Building and Environment, 237*, Article 110295.

Chen, Z., Dong, B., Pei, Q., & Zhang, Z. (2022a). The impacts of urban vitality and urban density on innovation: Evidence from China's Greater Bay Area. *Habitat International, 119*, Article 102490.

Chen, J., Gao, M., Cheng, S., Hou, W., Song, M., Liu, X., & Liu, Y. (2022b). Global 1 km× 1 km gridded revised real gross domestic product and electricity consumption during 1992–2019 based on calibrated nighttime light data. *Scientific Data, 9*(1), 202.

Chuah, P. L. (2020). Ghost towns. Revitalizing abandoned towns for sustainable and sharing community. *Master's thesis)*. http://hdl.handle.net/10589/167531. Politecnico di MILANO.

Constant, A. F., & Zimmermann, K. F. (2013). *International handbook on the economics of migration*. Edward Elgar Publishing.

Delclòs-Alió, X., & Miralles-Guasch, C. (2018). Looking at Barcelona through Jane Jacobs's eyes: Mapping the basic conditions for urban vitality in a Mediterranean conurbation. *Land Use Policy, 75*, 505–517.

Ding, X., Zhang, Y., Haick, H., & Zhang, M. (2025). Artificial intelligence-assisted data fusion. In *Nature-inspired sensors* (pp. 549–560). Elsevier.

Dong, L., Du, R., Kahn, M., Ratti, C., & Zheng, S. (2021). "Ghost cities" versus boom towns: Do China's high-speed rail new towns thrive? *Regional Science and Urban Economics, 89*, Article 103682.

Elvidge, C. D., Zhizhin, M., Ghosh, T., Hsu, F. C., & Taneja, J. (2021). Annual time series of global VIIRS nighttime lights derived from monthly averages: 2012 to 2019. *Remote Sensing, 13*(5), 922.

Ge, W., Yang, H., Zhu, X., Ma, M., & Yang, Y. (2018). Ghost city extraction and rate estimation in China based on NPP-VIIRS night-time light data. *ISPRS International Journal of Geo-Information, 7*, 219.

Gómez-Varo, I., Delclòs-Alió, X., & Miralles-Guasch, C. (2022). Jane Jacobs reloaded: A contemporary operationalization of urban vitality in a district in barcelona. *Cities, 123*, Article 103565.

Gong, P., et al. (2020). Annual maps of global artificial impervious area (GAIA) between 1985 and 2018. *Remote Sensing of Environment, 236*, Article 111510.

Gowharji, W. F. (2016). *A computational tool for evaluating urban vitality using Kendall Square development proposals as a case study*. Massachusetts Institute of Technology.

Gu, Y., et al. (2023). Generative design method of building group based on AIP (Aging in Place) assessment: The case of dense urban renewal districts in Hong Kong. In *World congress of architects* (pp. 479–495). Springer International Publishing. https://doi.org/10.1007/978-3-031-36302-3_35.

Guo, X., et al. (2022). Spatial social interaction: An explanatory framework of urban space vitality and its preliminary verification. *Cities, 121*, Article 103487.

Herfort, B., Lautenbach, S., Porto de Albuquerque, J., Anderson, J., & Zipf, A. (2023). A spatio-temporal analysis investigating completeness and inequalities of global urban building data in OpenStreetMap. *Nature Communications, 14*, 3985.

Huang, J., Cui, Y., Li, L., Guo, M., Ho, H. C., Lu, Y., & Webster, C. (2023). Re-examining Jane Jacobs' doctrine using new urban data in Hong Kong. *Environment and Planning B: Urban Analytics and City Science, 50*(1), 76–93.

Huang, B., et al. (2020). Evaluating and characterizing urban vibrancy using spatial big data: Shanghai as a case study. *Environ Plan B-urban, 47*, 1543–1559.

Jacobs, J. (1961). *The death and life of great American cities*. New York: Random House.

Jiang, S., Alves, A., Rodrigues, F., Ferreira, J., & Pereira, F. C. (2015). *Mining point-of-interest data from social networks for urban land use classification and disaggregation* (Vol. 53, pp. 36–46). Comput Environ Urban.

Jin, X., et al. (2017). Evaluating cities' vitality and identifying ghost cities in China with emerging geographical data. *Cities, 63*, 98–109.

Klinkhardt, C., et al. (2023). Quality assessment of OpenStreetMap's points of interest with large-scale real data. *Transportation Research Record, 2677*, 661–674.

Kropf, K. (2017). *The handbook of urban morphology*. New Jersey, NJ: Wiley.

Kumari, P. (2019). 20 of the most prominent ghost towns around the world that remain abandoned till date. https://www.scoopwhoop.com/travel/ghost-towns-around-the-world/.

Leichtle, T., Lakes, T., Zhu, X. X., & Taubenböck, H. (2019). *Has dongying developed to a ghost city? - evidence from multi-temporal population estimation based on VHR remote sensing and census counts* (Vol. 78). Comput Environ Urban, Article 101372.

Li, X., et al. (2020a). Mapping global urban boundaries from the global artificial impervious area (GAIA) data. *Environmental Research Letters, 15*, Article 094044.

Li, Y., et al. (2023). Greening the concrete jungle: Unveiling the co-mitigation of greenspace configuration on PM2.5 and land surface temperature with explanatory machine learning. *Urban Forestry and Urban Greening.* , Article 128086. https://doi.org/10.1016/j.ufug.2023.128086

Li, X., Zhou, Y., Zhao, M., & Zhao, X. (2020b). A harmonized global nighttime light dataset 1992–2018. *Scientific Data, 7*(1), 168.

Liu, H., et al. (2020). Annual dynamics of global land cover and its long-term changes from 1982 to 2015. *Earth System Science Data, 12*(2), 1217–1243.

Lloyd, C. T., et al. (2019). Global spatio-temporally harmonised datasets for producing high-resolution gridded population distribution datasets. *Big Earth Data, 3*(2), 108–139.

Long, Y., & Huang, C. (2019). Does block size matter? The impact of urban design on economic vitality for Chinese cities. *Environ Plan B-urban, 46*, 406–422.

Lynch, K. (1984). *Good city form*. MIT press.

O' Callaghan, C., Boyle, M., & Kitchin, R. (2014). Post-politics, crisis, and Ireland's 'ghost estates'. *Political Geography, 42*, 121–133.

Oostwegel, L. J. N., Ospina, N. G., Zadeh, T. E., Shinde, S., & Schorlemmer, D. (2023). Automatic global building completeness assessment of OpenStreetMap using remote sensing data. https://meetingorganizer.copernicus.org/EGU23/EGU23-13160.html.

Paköz, M. Z., Yaratgan, D., & Şahin, A. (2022). Re-mapping urban vitality through Jane Jacobs' criteria: The case of Kayseri, Turkey. *Land Use Policy, 114*, Article 105985.

Pinho, M. G. M., et al. (2023). The quality of OpenStreetMap food-related point-of-interest data for use in epidemiological research. *Health & Place, 83*, Article 103075.

PopGrid Data Collaborative. (2020). Leaving No one off the map: A guide for gridded population data for sustainable development. https://static1.squarespace.com/static/5b4f63e14eddec374f416232/t/5eb2b65ec575060f0adb1feb/1588770424043/Leaving+no+one+off+the+map-4.pdf.

Roger, S. A. (2011). The empty city of ordos, China: A modern ghost town. Retrieved from https://weburbanist.com/2011/01/10/the-empty-city-of-ordos-China-amodern-ghost-town/.

Shepard, W. (2015). *Ghost cities of China: The story of cities without people in the world's most populated country*. Bloomsbury Publishing.

Shi, L., et al. (2020). Urbanization that hides in the dark – spotting China's "ghost neighborhoods" from space. *Landscape and Urban Planning, 200*, Article 103822.

Stevens, F. R., Gaughan, A. E., Linard, C., & Tatem, A. J. (2015). Disaggregating census data for population mapping using random forests with remotely-sensed and ancillary data. *PLoS One, 10*, Article e0107042.

Store, C. C. D. (2019). Land cover classification gridded maps from 1992 to present derived from satellite observations. *Copernicus Climate Change Service, 7–9*.

Sung, H.-G., Go, D.-H., & Choi, C. G. (2013). Evidence of Jacobs's street life in the great Seoul city: Identifying the association of physical environment with walking activity on streets. *Cities, 35*, 164–173.

Tatem, A. J. (2017). WorldPop, open data for spatial demography. *Scientific Data, 4*, 1–4. https://doi.org/10.1038/sdata.2017.4

United Nation. (2015). United nations sustainable development action. https://www.un.org/sustainabledevelopment/cities/, 2015.

Wang, L., et al. (2012). China's urban expansion from 1990 to 2010 determined with satellite remote sensing. *Chinese Science Bulletin, 57*, 2802–2812.

Wang, L., Han, X., He, J., & Jung, T. (2022). Measuring residents' perceptions of city streets to inform better street planning through deep learning and space syntax. *ISPRS Journal of Photogrammetry and Remote Sensing, 190*, 215–230. https://doi.org/10.1016/j.isprsjprs.2022.06.011

Wang, L., Hou, C., Zhang, Y., & He, J. (2024). Measuring solar radiation and spatio-temporal distribution in different street network direction through solar trajectories and street view images. *International Journal of Applied Earth Observation and Geoinformation, 132*, Article 104058.

Williams, S., Xu, W., Tan, S. B., Foster, M. J., & Chen, C. (2019). Ghost cities of China: Identifying urban vacancy through social media data. *Cities, 94*, 275–285.

Wu, J., Ta, N., Song, Y., Lin, J., & Chai, Y. (2018). Urban form breeds neighborhood vibrancy: A case study using a GPS-based activity survey in suburban beijing. *Cities, 74*, 100–108.

Xia, C., Zhang, A., & Yeh, A. G. (2022). The varying relationships between multidimensional urban form and urban vitality in Chinese megacities: Insights from a comparative analysis. *Annals of the Association of American Geographers, 112*(1), 141–166.

Xu, B. (2022). China's new towns in controversy: A literature review. *Journal of Planning Literature, 37*, 236–248.

Xu, Z., et al. (2021). Mapping hierarchical urban boundaries for global urban settlements. *International Journal of Applied Earth Observation and Geoinformation, 103*, Article 102480.

Ye, Y., Li, D., & Liu, X. (2018). How block density and typology affect urban vitality: An exploratory analysis in shenzhen, China. *Urban Geography, 39*, 631–652.

Yue, W., et al. (2021). Identifying urban vitality in metropolitan areas of developing countries from a comparative perspective: Ho chi minh city versus shanghai. *Sustainable Cities and Society, 65*, Article 102609.

Zhang, X., et al. (2022a). Underload city conceptual approach extending ghost city studies. *Npj Urban Sustain, 2*, 1–10.

Zhang, Y., Zhang, Q., Zhao, Y., Deng, Y., Liu, F., & Zheng, H. (2022c). Artificial intelligence prediction of urban spatial risk factors from an epidemic perspective. In *The international conference on computational design and robotic fabrication* (pp. 209–222). Singapore: Springer Nature Singapore.

Zhang, Y., Zhang, Q., Zhao, Y., Deng, Y., & Zheng, H. (2022b). Urban spatial risk prediction and optimization analysis of POI based on deep learning from the perspective of an epidemic. *International Journal of Applied Earth Observation and Geoinformation, 112*, Article 102942. https://doi.org/10.1016/j.jag.2022.102942

Zhang, Y., Zhao, H., & Long, Y. (2024). CMAB: A first national-scale multi-attribute building dataset derived from open source data and GeoAI. *arXiv preprint arXiv: 2408.05891*.

Zheng, Q., et al. (2017). Monitoring and assessing "ghost cities" in Northeast China from the view of nighttime light remote sensing data. *Habitat International, 70*, 34–42.

Zheng, L., Long, F., Chang, Z., & Ye, J. (2019). Ghost town or city of hope? The spatial spillover effects of high-speed railway stations in China. *Transport Policy, 81*, 230–241.

Zhou, J. (2012). *Urban vitality in Dutch and Chinese new towns: A comparative study between almere and Tongzhou* (Vol. 3). Technische Universiteit Delft.

Zhou, Y., Li, X., Asrar, G. R., Smith, S. J., & Imhoff, M. (2018). A global record of annual urban dynamics (1992–2013) from nighttime lights. *Remote Sensing of Environment, 219*, 206–220.

Li, W., Zhang, Y., Li, M., & Long, Y. (2024). Rethinking the country-level percentage of population residing in urban area with a global harmonized urban definition. *iScience, 27*(6), 110125. https://doi.org/10.1016/j.isci.2024.110125.